

Alma Mater Studiorum Università di Bologna
Archivio istituzionale della ricerca

Quantum Effects for a Proton in a Low-Barrier, Double-Well Potential: Core Level Photoemission Spectroscopy of Acetylacetone

This is the final peer-reviewed author's accepted manuscript (postprint) of the following publication:

Published Version:

Quantum Effects for a Proton in a Low-Barrier, Double-Well Potential: Core Level Photoemission Spectroscopy of Acetylacetone / Feyer, Vitaliy; Prince, Kevin C.; Coreno, Marcello; Melandri, Sonia; Maris, Assimo; Evangelisti, Luca; Caminati, Walther; Giuliano, Barbara M.; Kjaergaard, Henrik G.; Carravetta, Vincenzo. - In: THE JOURNAL OF PHYSICAL CHEMISTRY LETTERS. - ISSN 1948-7185. - STAMPA. - 9:3(2018), pp. 521-526. [10.1021/acs.jpcllett.7b03175]

Availability:

This version is available at: <https://hdl.handle.net/11585/622716> since: 2020-02-27

Published:

DOI: <http://doi.org/10.1021/acs.jpcllett.7b03175>

Terms of use:

Some rights reserved. The terms and conditions for the reuse of this version of the manuscript are specified in the publishing policy. For all terms of use and more information see the publisher's website.

This item was downloaded from IRIS Università di Bologna (<https://cris.unibo.it/>).
When citing, please refer to the published version.

(Article begins on next page)

This is the final peer-reviewed accepted manuscript of:

**Quantum Effects for a Proton in a Low-barrier, Double-well Potential:
Core Level Photoemission Spectroscopy of Acetylacetone.**

**V. Feyer, K.C. Prince, M. Coreno, S. Melandri, A. Maris, L. Evangelisti,
W. Caminati, B.M. Giuliano, H.G. Kjaergaard, V. Carravetta.**

The Journal of Physical Chemistry Letters 9 (2018) 521-526

**The final published version is available online at:
<https://doi.org/10.1021/acs.jpcllett.7b03175>**

Rights / License:

**The terms and conditions for the reuse of this version of the manuscript
are specified in the publishing policy.
For all terms of use and more information see the publisher's website.**

Quantum Effects for a Proton in a Low-Barrier, Double-Well Potential: Core Level Photoemission Spectroscopy of Acetylacetonone

Vitaliy Feyer,[†] Kevin C. Prince,^{*,†} Marcello Coreno,[§] Sonia Melandri,[‡] Assimo Maris,[‡] Luca Evangelisti,[‡] Walther Caminati,[‡] Barbara M. Giuliano,[¶] Henrik G. Kjaergaard,[#] and Vincenzo Carravetta^{||}

[†]Elettra-Sincrotrone Trieste, in Area Science Park, I-34149 Trieste, Italy

[‡]Molecular Model Discovery Laboratory, Department of Chemistry and Biotechnology, Swinburne University of Technology, 3122 Melbourne, Australia

[§]ISM-CNR—Istituto di Struttura della Materia, LD2 unit, I-34149 Trieste, Italy

[‡]Dipartimento di Chimica, “G. Ciamician” dell’Università, I-40126 Bologna, Italy

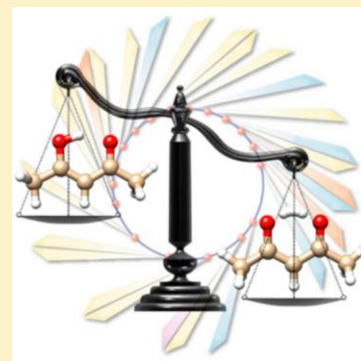
[¶]Departamento de Química, Universidade de Coimbra, 3004-535 Coimbra, Portugal

[#]Department of Chemistry, University of Copenhagen, 2100 Copenhagen, Denmark

^{||}ISM-CNR, Institute of Chemical Physical Processes, I-56124 Pisa, Italy

^{*} Supporting Information

ABSTRACT: We have performed core level photoemission spectroscopy of gaseous acetylacetonone, its fully deuterated form, and two derivatives, benzoylacetone and dibenzoylmethane. These molecules show intramolecular hydrogen bonds, with a proton located in a double-well potential, whose barrier height is different for the three compounds. This has allowed us to examine the effect of the double-well potential on photoemission spectra. Two distinct O 1s core hole peaks are observed, previously assigned to two chemical states of oxygen. We provide an alternative assignment of the double-peak structure of O 1s spectra by taking full account of the extended nature of the wave function associated with the nuclear motion of the proton, the shape of the ground and final state potentials in which the proton is located, and the nonzero temperature of the samples. The peaks are explained in terms of an unusual Franck–Condon factor distribution.



Hydrogen bonding (HB) is ubiquitous in biology and of fundamental importance in many fields of physics and chemistry, from the apparently simple case of water to the undoubtedly complex cases of DNA structure and protein folding.^{1–3} In condensed matter, analysis of HB is complex, but it becomes more tractable in isolated molecules. Computational modeling of molecules always requires some approximations, and nuclear motion is commonly described by molecular dynamics with the assumptions of the Born–Oppenheimer (BO) approximation and classical behavior. This is at the cost of neglecting the quantum mechanical nature of HB, particularly nuclear quantum effects, which we show may be of crucial importance. The molecular systems chosen here (see Figure 1) allow us to examine this aspect and to give a fuller description of quantum effects in intramolecular HB. We report here a study of the hydrogen-bonded systems acetylacetonone (ACAC), benzoylacetone (BAC), and dibenzoylmethane (DBM), Figure 1.

The symmetric β -diketones belong to the class of systems in which the HB can be locally described as $X_1-H \cdots X_2$ (X_1 and X_2 are atoms of the same element), and the proton can be transferred, resulting in two equivalent tautomers. Historically,

the main experimental techniques used to investigate the structure of ACAC and its derivatives have been nuclear magnetic resonance (NMR),^{4–8} infrared,^{9–15} and microwave spectroscopy,¹⁶ as well as structural techniques including electron, X-ray, and neutron diffraction.^{17–22} The general consensus^{5,20,21} is that the bridging hydrogen in ACAC exists in a double-minimum potential, with the ground state below the maximum and C_s symmetry. Another view, based on microwave spectroscopy and one calculation, is that the symmetry is in fact C_{2v} .^{16,23} Theoretical calculations of the ground state of ACAC at different levels of accuracy^{13–15,23–27} assessed the shape of the PES (potential energy surface) with respect to the movement of the enol hydrogen. The most accurate calculations, by the coupled cluster including singles and doubles and perturbative triples [CCSD(T)] method²⁶ confirmed that the PES can be described as a double well, with the minima corresponding to a C_s structure, the H atom forming a bond with either O atom, and a rather low energy

Received: November 30, 2017

Accepted: January 9, 2018

Published: January 9, 2018

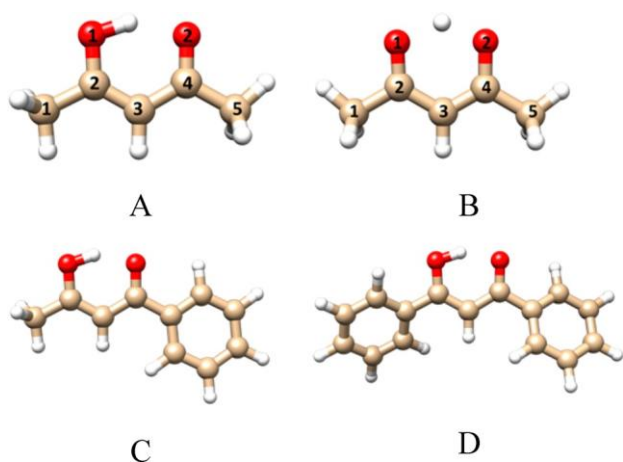


Figure 1. Schematic structures of (A) ACAC in C_s configuration, (B) ACAC in C_{2v} configuration, “geometry 0” in the text, (C) BAC, and (D) DBM. Colors indicate atoms: red, oxygen; beige, carbon; white, hydrogen.

barrier.²⁶ These authors predicted a value of 15 kJ/mol for the highest-level calculations. In a study using the same theoretical model and including IR spectroscopy study, calculations indicated a barrier of 13.4 kJ/mol, while the position of the OH-stretching fundamental implied a barrier of ca. 10 kJ/mol.¹⁵ For DBM, ¹³C NMR studies⁶ indicate that the oxygen atoms are equivalent in solution, i.e., the bridging hydrogen is symmetrically located while the oxygen atoms are slightly inequivalent in the solid state. Thomas et al.²² examined DBM in the solid state, noting that neutron and X-ray diffraction provided different structural information because neutron diffraction is sensitive to the nuclear position while X-ray diffraction is sensitive to the electron density. Neutron diffraction indicated an asymmetric location of the proton between the two oxygen atoms, and the position was invariant between 100 and 280 K. The electron density, however, moved from an asymmetric distribution to nearly central at 280 K. In the gas phase at higher temperature than these measurements (as in the present work), we expect that the molecule is more symmetric. Gilli et al.² concluded that DBM possesses a symmetric well with no barrier to hydrogen movement. From these and other studies, it appears that the free molecule is symmetric, with the bridging hydrogen atom located on average at the center.

For BAC, X-ray and neutron scattering^{28,29} at low temperature indicated that the keto–enol group is rather symmetric in the solid state and that the hydrogen is located in a wide, flat potential. Again, we expect that in the gas phase at room temperature the system is more symmetric due to thermal fluctuations; Gilli et al.² concluded that it was a low-barrier, asymmetric, double-well system. We note in passing that a double well may arise not only when the reaction coordinate is along the bond but also when it is the bond angle.^{29,30}

Most of these calculations or interpretations of experimental data of gas phase molecules did not address quantum nuclear effects (QNEs), which derive from the delocalized wave function of the proton. However, Tuckerman et al.,³¹ in a theoretical study pointed out that not only is the quantum nature of the proton relevant but also that of the heavy atoms in a molecule such as malonaldehyde.³² In condensed matter, and for intermolecular rather than intramolecular HB, Li et al.³³ found that inclusion of QNEs in calculations makes weak HBs

weaker, but strong HBs become even stronger, while for water layers on metals, a strong delocalization of the protons was found.³⁴

Here we consider the effect of QNEs on both the structure of our samples and our measurement technique, core level photoemission spectroscopy. The effect of intermolecular HB on this spectroscopy has been studied in the related case of the water dimer, where the bond is much weaker.³⁵ A fundamental idea underlying electron spectroscopy is that photoelectrons from the same element, and having different energies, originate from atoms in different chemical environments in the ground state. Some exceptions are known to this rule, for example, in condensed matter physics, carbon monoxide adsorbed on Cu and Ag surfaces^{36–39} gives rise to up to three C and O 1s peaks, although only a single chemical state is present. These peaks are described as screened and unscreened, corresponding to electron transfer (or its absence) from the substrate to the molecule. We return to this point in the discussion.

The O core level spectra of the samples are shown in Figure 2, and the data are summarized in Table 1. The relative

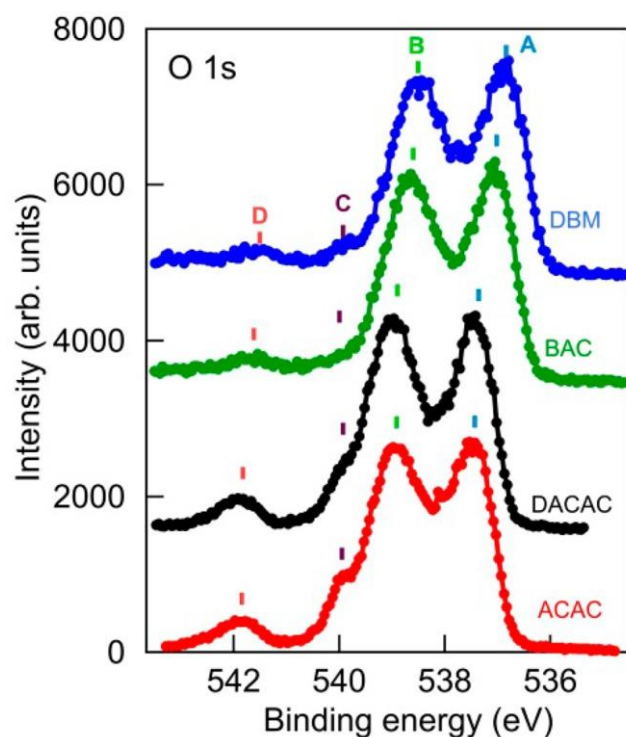


Figure 2. Experimental O 1s spectra of (top to bottom) DBM, BAC, DACAC, and ACAC.

intensities were obtained by fitting the spectra with Gaussian profiles. The O 1s spectra all consist of two main peaks labeled A and B, a shoulder C, and a weak peak D. Peak C is assigned to photoemission from residual water in the vacuum (binding energy 539.8 eV⁴⁰) and peak D to satellite states. The core electron binding energies in ACAC and DACAC are equal within experimental error, and the main difference is the deeper valley between the two peaks of DACAC. The corresponding energies of BAC and DBM are 0.3–0.5 eV lower than those of ACAC due to additional final state screening by the phenyl moieties. Peaks A and B were assigned previously to enolic and ketonic oxygen⁴¹ and are in good agreement with a recent

Table 1. Experimental O 1s Binding Energies (BE/eV) and Relative Intensities (I)

	ACAC		DACAC		DBM		BAC	
	BE/BE/BE/BE/							
peak A	537.5	0.35	537.45	0.37	536.9	0.37	537.1	0.37
peak B	538.9	0.55	539.0	0.54	538.5	0.50	538.6	0.51
peak C	540.1	0.03	540.15	0.03	540.0	0.02	540.2	0.02
peak D	541.9	0.07	541.9	0.06	541.6	0.11	541.7	0.10

theoretical study,⁴² but our calculations suggest an alternative assignment.

First we discuss ACAC and DACAC and consider BAC and DBM later. To analyze the effect of nuclear motion, we reduce the complicated dynamics of these polyatomic molecules to a simplified one-dimensional model that focuses on the motion of interest. Moreover, we have carried out calculations for ACAC and DACAC only, which are computationally more tractable than the other molecules. We consider only the motion of the proton between the two fixed oxygen atoms of ACAC, with the heavy atoms in a planar structure. To get a one-dimensional potential curve for the motion of H, we optimized, with DFT-B3LYP/aug-cc-pVDZ calculations, the geometry in which H is kept equidistant from the two oxygen atoms and the heavy atom backbone is kept planar. This C_{2v} geometry with the methyl groups in eclipsed configuration is a stationary point and is denoted “geometry 0”. The one-dimensional path of the proton along the lines joining the H position at 0 and the two nuclei of oxygen is then defined by these two lines, forming an angle of about 150° , with negative displacements when the proton is closer to the left oxygen (O1) in Figure 1. For a number of positions of H along this coordinate, both HF and DFT-B3LYP partial optimizations of the initial state were performed, keeping H and the oxygen atoms fixed. Moving the H atom reduces the symmetry to C_s , and the partial geometry optimization does not alter this symmetry, which is maintained at each position. We believe that the essential quantum mechanical behavior of the O 1s core spectra can still be understood with this simplification for the nuclear motion.

The result of the HF calculations in the BO diabatic approximation, neglecting vibronic coupling, is the set of potential energy curves (PES, heavy line) in Figure 3; the DFT-B3LYP calculations lead to a PES of essentially the same shape. The ground state PES (green line) is symmetrical about 0, with two weak minima corresponding to the formation of a covalent bond between an oxygen atom and H. The two minima are separated by a barrier of 36 kJ/mol, in agreement with previous all-nuclei calculations at the HF level,²⁴ validating our model. Solving the problem of the vibrational motion of the proton in this double-well potential, we obtain the ground state wave function shown in Figure 3, lower panel. Due to the very low barrier, the vibrational wave function has two barely visible maxima corresponding to the two minima of the PES, but it is largely delocalized. The semiclassical picture that the proton moves essentially around positions corresponding to a covalent bond with one oxygen atom and a hydrogen bond with the other oxygen atom, yielding two chemically different oxygen atoms, is difficult to justify when we use a quantum description of the H motion. Considering only the initial vibrational state, we may expect a spectrum with a very broad O 1s band due to the substantial delocalization of the proton. For core ionization, the electronic relaxation is fast (sudden approximation) and the

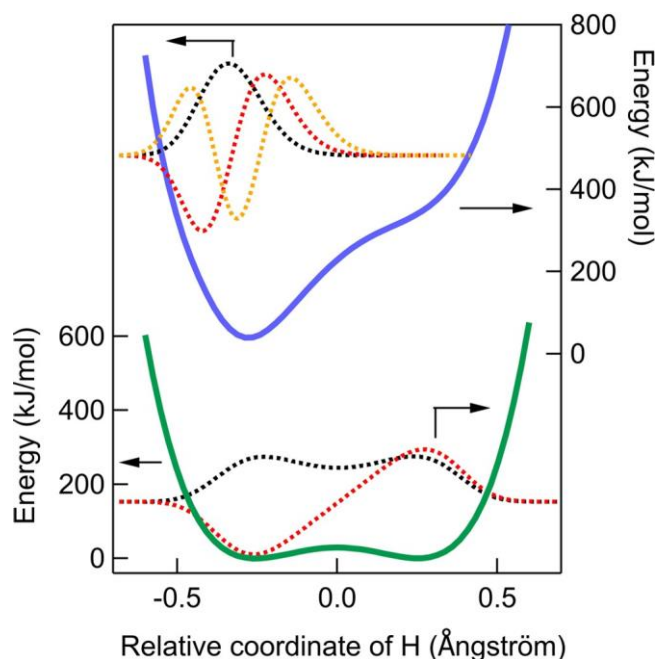


Figure 3. Left and right axes: potential curves of ACAC in the ground state (PES-gs, thick green curve) and core ionized state (PES-ion, thick blue curve). The amplitudes of the vibrational wave functions (in arbitrary units, scale not shown) for the ground states (black curves), the first excited states (red curves), and the second excited state (yellow curve) of the proton in the ground/core ionized states are also shown.

XPS spectrum reflects the structure of the final vibrational state (Franck–Condon (FC) principle).

We performed HF calculations⁴³ for the electronic ground state of the O 1s ion with a localized core hole^{44,45} on one of the oxygen atoms, O2. The same geometries as those of the PES of the neutral ground state were used to calculate the ionic state: the result is the PES (heavy blue line) in Figure 3, denoted PES-ion. The PES-ion is strongly asymmetric; for negative values of the proton coordinate, its form is similar to that of the PES-gs, but for positive values of the H coordinate, a strongly repulsive potential for the proton is added to the PES-gs. This is because at positive values of the position, the proton is nearer the ionized O2 atom, and the hole generates a repulsive potential for the proton. The finer details of the two PES computed for ACAC may depend on the simplified, one-dimensional model adopted and on the quality of the calculations, but their shape is essentially that in Figure 3.

To test the effect of barrier height on our results, we slightly modified our PES-gs computed by HF calculations by using the value of 15 kJ/mol obtained by the more accurate CCSD(T) calculations;²⁶ the difference (not shown) between the wave function obtained with the corrected PES and the HF PES (black line in Figure 3) is negligible. The particular shape of the

PES-ion leads to vibrational wave functions that tend to be localized at negative values of the relative coordinate of H but that also tend to shift toward positive values as the vibrational energy increases. This gives rise to a distribution of FC factors that, in the BO approximation, describe how the initial wave function of the proton is projected on the final state wave functions and is rather special, as shown in Figure 4. The

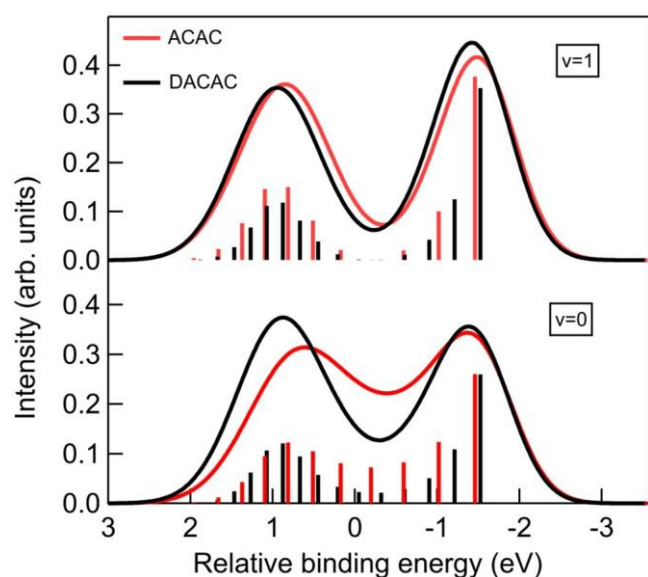


Figure 4. Theoretical O 1s core level spectra of ACAC (red curves) and DACAC (black curves) in the ground (lower panel) and first vibrational (upper panel) states. E_v is the vibrational energy of the electronic ground state. The discrete spectra (histograms) have been convoluted with Gaussian functions of $\text{fwhm} = 1$ eV to generate the curves.

spectral profile (histogram) and its convolution (line) may be sensitive to the finer details of the PES-ion but shows qualitatively that the particular shape of the PES-ion can lead to an XPS spectrum very similar to that measured. The same calculations for the deuterated molecule DACAC (black histograms and lines, Figure 4, lower panel) reproduce the main difference observed with respect to the spectrum of ACAC, that is, the reduced intensity in the valley between the two bands. Because of the low-energy barrier, two vibrational levels ($v=0$, 884 cm^{-1} and $v=1$, 1126 cm^{-1}) with an energy difference of about 2.87 kJ/mol are populated at the experimental temperature (300 K), with a population ratio of $1:0.32$. However, the normal and “hot” bands reported in Figure 4 show similar behavior, and the population of the $v=1$ level does not affect our analysis. This theoretical interpretation is not quantitative but explains the main characteristics of the XPS spectra in terms of an effect of the special initial and final state PES.

Additional support for our conclusion of the high symmetry of ACAC is provided by the C 1s spectrum; see the Supporting Information. Briefly, calculations for C_s geometry predict an additional splitting in the spectra, which is not observed experimentally, and the data are more consistent with C_{2v} symmetry.

Turning now to BAC and DBM, we noted above the general consensus that the energy barrier in the PES-gs is very low or zero, so that the two O atoms have the same bonding environments in the ground states. However, their experimental

O 1s spectra are quite similar to that of ACAC, with only a rigid shift (due to additional screening), thus supporting the view that for double-well systems there is an alternative explanation for the double peaks in the XPS spectra. For these two molecules, we can reasonably expect that by adopting the same approximations introduced for ACAC the one-dimensional gs and O 1s ion state PESs for the H motion have essentially the same structure presented in Figure 3, and consequently, the corresponding FC distributions will be similar to that of ACAC in Figure 4. We conclude that when the energy barrier is just a few kJ/mol , the point-like description of the proton is no longer valid and the structural concept of the molecule should be revised to take account of the strongly delocalized nuclear wave function. From the structure of the heavy atom skeleton and the form of the gs vibrational wave function (Figure 3) for the H, we suggest that C_{2v} instead of C_s should be the preferred symmetry label for ground electronic state ACAC, especially if it is vibrationally excited.

The O 1s spectrum of ACAC can apparently be explained by the conventional chemical shift model. However, our theoretical calculations suggest that an unusual FC distribution derived from the strongly asymmetric structure of the final state potential, coupled with the delocalization of the proton in the ground state, gives an equally good description for ACAC and a better one for BAC and DBM spectra. As mentioned above, this process is in some ways analogous to the case of CO molecules adsorbed on copper and silver substrates.^{36–39} In those systems, the molecule has a single chemical state, but the carbon and oxygen core levels show three separate peaks, with two peaks having comparable intensity. The difference between the final states is that electrons are localized in different orbitals. Similarly, in the three compounds considered here, the unusually large delocalization of the proton in the ground state gives rise to an unexpected FC distribution, and it may localize in different positions in the final state. The approximately equal intensities of the measured peaks indicate qualitatively that the probability in the initial state of finding the hydrogen atom “near” or “far from” the hole is about equal. In other words, the initial state wave function, which determines the probable position of the atom, is spread over a broad volume, as confirmed by the present calculations. The good agreement between theory and experiment and the similarity of the ACAC, DBM, and BAC spectra imply that the local molecular symmetry of the oxygen–hydrogen–oxygen atoms for this spectroscopic technique is effectively C_{2v} for the first two compounds and C_{2v} -like for (asymmetric) BAC. Data for deuterated DACAC (the deeper minimum in Figure 4) support our conclusions. Finally, these results suggest a re-evaluation of photoemission results from condensed matter when the same quantum effects of HB are present.^{33,34}

EXPERIMENTAL AND COMPUTATIONAL METHODS

The experiments were performed at the Gas Phase Photoemission beamline at the synchrotron light source Elettra, Trieste, Italy, using the apparatus, photon energies, resolution, and calibration procedure described previously.⁴⁶ ACAC (purity > 99%), DBM (purity > 98%), and BAC (purity > 99%) were purchased from Sigma-Aldrich, ACAC-*d*8 (98% D) was purchased from Cambridge Isotope Laboratories, and all compounds were used without further purification. ACAC and DACAC were introduced into the system via a heatable effusive needle source. Before introducing DACAC, the gas inlet system

was conditioned with heavy water to avoid proton–deuterium exchange on surfaces, and the isotopic purity was monitored with a quadrupole mass spectrometer in the chamber. BAC and DBM were evaporated from a crucible. An ambient temperature of 297 K produced a background pressure of BAC of 1.5×10^{-5} mbar, which was sufficient for measurements. DBM was heated to 355 K.

The calculations of the initial (gs) and final (core hole) PESs were performed at the HF and DFT levels (B3LYP functional⁴³) with the aug-cc-pVDZ basis set. The DALTON program,⁴⁵ where a maximum overlap criterion⁴⁷ is implemented to avoid variational collapse of the core hole state, was employed. The one-dimensional Schrödinger equation (see below) for the motion of H in the initial and final PESs was solved numerically by the Numerov method.⁴⁸ The Δ_{HF} method employed for the calculation of core binding energies includes the important electron relaxation effect, beyond the Koopman theorem, and neglects the relatively small differential electron correlation energy. This approach has proved to be quite accurate for the prediction of core level chemical shifts (see, for instance, ref 46).

ASSOCIATED CONTENT

Supporting Information

The Supporting Information is available free of charge on the ACS Publications website at DOI: 10.1021/acs.jpcllett.7b03175.

Description of the experimental carbon 1s core level spectra, their theoretical calculation, and their assignment (PDF)

AUTHOR INFORMATION

Corresponding Author

*E-mail: Prince@Elettra.eu.

ORCID

Vitaliy Feyrer: 0000-0002-7104-5420

Kevin C. Prince: 0000-0002-5416-7354

Assimo Maris: 0000-0003-2644-0023

Luca Evangelisti: 0000-0001-9119-1057

Henrik G. Kjaergaard: 0000-0002-7275-8297

Present Addresses

V.F.: Forschungszentrum Jülich GmbH, Peter Grünberg

Institute, Electronic Properties (PGI-6), 52425 Jülich, Germany.

°B.M.G.: Max-Planck-Institut für extraterrestrische Physik, 85748 Garching bei München, Germany.

Notes

The authors declare no competing financial interest.

ACKNOWLEDGMENTS

The research leading to these results received funding from the European Community's Seventh Framework Programme (FP7/2007-2013) under grant agreement n°226716. M.C. acknowledges support from the "Ministero della Istruzione, della Università e della Ricerca" of the Republic of Italy (Project FIRB No. RBID08CRXK and PRIN 2010ERFKXL_006). We thank our colleagues at Elettra for their support and the provision of high-quality synchrotron light.

REFERENCES

(1) Moore, T. S.; Winmill, T. F. The State of Amines in Aqueous Solution. *J. Chem. Soc., Trans.* 1912, 101, 1635–1676.

(2) Gilli, P.; Bertolasi, V.; Pretto, L.; Ferretti, V.; Gilli, G. Covalent versus Electrostatic Nature of the Strong Hydrogen Bond: Discrimination among Single, Double, and Asymmetric Single-Well Hydrogen Bonds by Variable-Temperature X-ray Crystallographic Methods in β -Diketone Enol RAHB Systems. *J. Am. Chem. Soc.* 2004, 126, 3845–3855.

(3) Arunan, E.; Desiraju, G. R.; Klein, R. A.; Sadlej, J.; Scheiner, S.; Alkorta, I.; Clary, D. C.; Crabtree, R. H.; Dannenberg, J. J.; Hobza, P.; Kjaergaard, H. G.; Legon, A. C.; Mennucci, B.; Nesbitt, D. J. Defining the Hydrogen Bond: An Account. *Pure Appl. Chem.* 2011, 83, 1619–36.

(4) Burdett, J. L.; Rogers, M. T. Keto-Enol Tautomerism in β -Dicarbonyls Studied by Nuclear Magnetic Resonance Spectroscopy. I. Proton Chemical Shifts and Equilibrium Constants of Pure Compounds. *J. Am. Chem. Soc.* 1964, 86, 2105–2109.

(5) Claramunt, R. M.; Lopez, C.; Santa María, M. D.; Sanz, D.; Elguero, J. The Use of NMR Spectroscopy to Study Tautomerism. *Prog. Nucl. Magn. Reson. Spectrosc.* 2006, 49, 169–206.

(6) Vila, A. J.; Lagier, C. M.; Olivieri, A. C. ¹³C NMR and AM1 Study of the Intramolecular Proton Transfer in Solid 1,3-Diphenylpropane-1,3-dione. *J. Chem. Soc., Perkin Trans.* 2 1990, 2, 1615–1618.

(7) Folkendt, M. M.; Weiss-Lopez, B. E.; Chauvel, J. P., Jr.; True, N. S. Gas-Phase ¹H NMR Studies of Keto-Enol Tautomerism of Acetylacetone, Methyl Acetoacetate, and Ethyl Acetoacetate. *J. Phys. Chem.* 1985, 89, 3347–3352.

(8) Kong, X.; Brinkmann, A.; Terskikh, V.; Wasylishen, R. E.; Bernard, G. M.; Duan, Z.; Wu, Q.; Wu, G. Proton Probability Distribution in the O···H···O Low-Barrier Hydrogen Bond: A Combined Solid-State NMR and Quantum Chemical Computational Study of Dibenzoylmethane and Curcumin. *J. Phys. Chem. B* 2016, 120, 11692–11704.

(9) Tayyari, S. F.; Milani-nejad, F. Vibrational Assignment of Acetylacetone. *Spectrochim. Acta, Part A* 2000, 56, 2679–2691.

(10) Chiavassa, T.; Verlaque, P.; Pizzala, L.; Roubin, P. Vibrational Studies of Methyl Derivatives of Malonaldehyde: Determination of a Reliable Force Field For β -Dicarbonyl Compounds. *Spectrochim. Acta* 1994, 50, 343–351.

(11) Emsley, J.; Ma, L. Y. Y.; Bates, P. A.; Hursthouse, M. B. β -diketone interactions: Part 7. X-Ray Molecular Structure of 3-(4'-Biphenyl)Pentane-2,4-Dione Reveals an Enol Tautomer with A very Strong Hydrogen Bond. *J. Mol. Struct.* 1988, 178, 297–299.

(12) Lozada-García, R. R.; Ceponkus, J.; Chin, W.; Chevalier, M.; Crepin, C. Acetylacetone in Hydrogen Solids: IR Signatures of the Enol and Keto Tautomers and UV Induced Tautomerization. *Chem. Phys. Lett.* 2011, 504, 142–147.

(13) Matanovic, I.; Doslic, N. Infrared Spectroscopy of the Intramolecular Hydrogen Bond in Acetylacetone: A Computational Approach. *J. Phys. Chem. A* 2005, 109, 4185–4194.

(14) Matanovic, I.; Doslic, N. Anharmonic Vibrational Spectra of Acetylacetone. *Int. J. Quantum Chem.* 2006, 106, 1367–1374.

(15) Howard, D. L.; Kjaergaard, H. G.; Huang, J.; Meuwly, M. Infrared and Near-infrared Spectroscopy of Acetylacetone and Hexafluoroacetylacetone. *J. Phys. Chem. A* 2015, 119, 7980–7990.

(16) Caminati, W.; Grabow, J.-U. The C_{2v} Structure of Enolic Acetylacetone. *J. Am. Chem. Soc.* 2006, 128, 854–857.

(17) Jones, R. D. G. The Crystal Structure of the Enol Tautomer of 1,3-Diphenyl-1,3-Propanedione (Dibenzoylmethane) by Neutron Diffraction. *Acta Crystallogr., Sect. B: Struct. Crystallogr. Cryst. Chem.* 1976, 32, 1807–1811.

(18) Etter, M. C.; Jahn, D. A.; Urbančzyk-Lipkowska, Z. A New Polymorph of Dibenzoylmethane. *Acta Crystallogr., Sect. C: Cryst. Struct. Commun.* 1987, 43, 260–263.

(19) Kaitner, B.; Meštrović, E. Structure of a New Crystal Modification of 1,3-diphenyl-1,3-propanedione. *Acta Crystallogr., Sect. C: Cryst. Struct. Commun.* 1993, 49, 1523–1525.

(20) Srinivasan, R.; Feenstra, J. S.; Park, S. T.; Xu, S.; Zewail, A. H. Direct Determination of Hydrogen-Bonded Structures in Resonant and Tautomeric Reactions Using Ultrafast Electron Diffraction. *J. Am. Chem. Soc.* 2004, 126, 2266–2267.

- (21) Boese, R.; Antipin, M. Yu.; Blaser, D.; Lyssenko, K. A. Molecular Crystal Structure of Acetylacetone at 210 and 110 K: Is the Crystal Disorder Static or Dynamic? *J. Phys. Chem. B* 1998, **102**, 8654.
- (22) Thomas, L. H.; Florence, A. J.; Wilson, C. C. Hydrogen Atom Behaviour Imaged in a Short Intramolecular Hydrogen Bond Using the Combined Approach of X-Ray and Neutron Diffraction. *New J. Chem.* 2009, **33**, 2486–2490.
- (23) Dannenberg, J. J.; Rios, R. Theoretical Study of the Enolic Forms of Acetylacetone. How Strong Is the H-Bond? *J. Phys. Chem.* 1994, **98**, 6714–6718.
- (24) Pakiari, A. H.; Eskandari, K. The Chemical Nature of Very Strong Hydrogen Bonds in Some Categories of Compounds. *J. Mol. Struct.: THEOCHEM* 2006, **759**, 51–60.
- (25) Chou, Y. C. Group-theoretical Investigation of the Tunneling Splitting Patterns of Enolic Acetylacetone. *J. Mol. Spectrosc.* 2010, **263**, 34–43.
- (26) Broadbent, S. A.; Burns, L. A.; Chatterjee, C.; Vaccaro, P. H. Investigation of Electronic Structure and Proton Transfer in Ground State Acetylacetone. *Chem. Phys. Lett.* 2007, **434**, 31–37.
- (27) Dolati, F.; Tayyari, S. F.; Vakili, M.; Wang, Y. A. Proton Transfer in Acetylacetone and Its α -Halo Derivatives. *Phys. Chem. Chem. Phys.* 2016, **18**, 344–350.
- (28) Madsen, G. K. H.; Iversen, B. B.; Larsen, F. K.; Kapon, M.; Reisner, G. M.; Herbstein, F. H. Topological Analysis of the Charge Density in Short Intramolecular O–H•••O Hydrogen Bonds. Very Low Temperature X-ray and Neutron Diffraction Study of Benzoylacetone. *J. Am. Chem. Soc.* 1998, **120**, 10040–10045.
- (29) Jones, R. D. G. The Crystal and Molecular Structure of the Enol Form of 1-Phenyl-1,3-butanedione (Benzoylacetone) by Neutron Diffraction. *Acta Crystallogr., Sect. B: Struct. Crystallogr. Cryst. Chem.* 1976, **32**, 2133–2136.
- (30) Ågren, H.; Reineck, I.; Veenhuizen, H.; Maripuu, R.; Arneberg, R.; Karlsson, L. A Theoretical Investigation of the U.V. Excited $^1A_1 \rightarrow ^2A_1$ Photoelectron Spectra of NH_3 and ND_3 . *Mol. Phys.* 1982, **45**, 477–492.
- (31) Tuckerman, M. E.; Marx, D.; Klein, M. L.; Parrinello, M. On the Quantum Nature of the Shared Proton in Hydrogen Bonds. *Science* 1997, **275**, 817–820.
- (32) Tuckerman, M. E.; Marx, D. Heavy-atom Skeleton Quantization and Proton Tunneling in “Intermediate-Barrier” Hydrogen Bonds. *Phys. Rev. Lett.* 2001, **86**, 4946–4949.
- (33) Li, X. Z.; Walker, B.; Michaelides, A. Quantum Nature of the Hydrogen Bond. *Proc. Natl. Acad. Sci. U. S. A.* 2011, **108**, 6369–6373.
- (34) Li, X. Z.; Probert, M. I. J.; Alavi, A.; Michaelides, A. Quantum Nature of the Proton in Water-Hydroxyl Overlayers on Metal Surfaces. *Phys. Rev. Lett.* 2010, **104**, 066102.
- (35) Felicissimo, V. C.; Minkov, I.; Guimaraes, F. F.; Gel'mukhanov, F.; Cesar, A.; Ågren, H. A Theoretical Study of the Role of the Hydrogen Bond on Core Ionization of the Water Dimer. *Chem. Phys.* 2005, **312**, 311–318.
- (36) Krause, S.; Mariani, C.; Prince, K. C.; Horn, K. Screening Effects in Photoemission from Weakly Bound Adsorbates: CO on Ag(110). *Surf. Sci.* 1984, **138**, 305–318.
- (37) Gunnarsson, O.; Schönhammer, K. CO on Cu(100) Explanation of the Three-Peak Structure in the X-Ray-Photoemission-Spectroscopy Core Spectrum. *Phys. Rev. Lett.* 1978, **41**, 1608–1612.
- (38) Bagus, P. S.; Seel, M. Molecular-orbital Cluster-Model Study of the Core-Level Spectrum of CO Adsorbed on Copper. *Phys. Rev. B: Condens. Matter Mater. Phys.* 1981, **23**, 2065–2075.
- (39) Messmer, R. P.; Lamson, S. H.; Salahub, D. R. Interpretation of Satellite Structure in the X-Ray Photoelectron Spectra of CO Adsorbed on Cu(100). *Phys. Rev. B: Condens. Matter Mater. Phys.* 1982, **25**, 3576–3592.
- (40) Sankari, R.; Ehara, M.; Nakatsuji, H.; Senba, Y.; Hosokawa, K.; Yoshida, H.; De Fanis, A.; Tamenori, Y.; Aksela, H.; Ueda, K. Vibrationally Resolved O 1s Photoelectron Spectrum of Water. *Chem. Phys. Lett.* 2003, **380**, 647–653.
- (41) Brown, R. S.; Tse, A.; Nakashima, T.; Haddon, R. C. Symmetries of Hydrogen-Bonded Enol Forms of Diketones as Determined by X-ray Photoelectron Spectroscopy. *J. Am. Chem. Soc.* 1979, **101**, 3157–3162.
- (42) Capron, N.; Casier, B.; Sisourat, N.; Piancastelli, M. N.; Simon, M.; Carniato, S. Probing Keto–enol Tautomerism Using Photoelectron Spectroscopy. *Phys. Chem. Chem. Phys.* 2015, **17**, 19991–19996.
- (43) Becke, A. D. A. New Mixing of Hartree-Fock and Local Density-Functional Theories. *J. Chem. Phys.* 1993, **98**, 5648–5642.
- (44) Bagus, P. S. Self-consistent-field Wave Functions for Hole States of Some Ne-Like and Ar-like Ions. *Phys. Rev.* 1965, **139**, A619–A634.
- (45) Angeli, C.; Bak, K. L.; Bakken, V.; Christiansen, O.; Cimiraglia, R.; Coriani, S.; Dahle, P.; Dalskov, E. K.; Enevoldsen, T.; Fernandez, B.; et al. *Dalton*, a molecular electronic structure program, release 2.0. <http://daltonprogram.org/> (2005).
- (46) Feyer, V.; Plekan, O.; Richter, R.; Coreno, M.; Prince, K. C.; Carravetta, V. A. Core Level Study of Alanine and Threonine. *J. Phys. Chem. A* 2008, **112**, 7806–7815.
- (47) Ågren, H.; Carravetta, V. The Core Electron Shake Phenomenon. *Int. J. Quantum Chem.* 1992, **42**, 685–718.
- (48) Johnson, B. R. New Numerical Methods Applied to Solving the One-Dimensional Eigenvalue Problem. *J. Chem. Phys.* 1999, **67**, 4086–4093.